Mon. Not. R. Astron. Soc. **000**, 1–?? (2002) Printed 18 November 2014 (MN LATEX style file v2.2)

# Discovery of a Quasi-Periodic Oscillation in the Ultraluminous X-ray Source IC 342 X-1: *XMM-Newton Results*

V. K. Agrawal[1⋆] and Anuj Nandi[1]
[1] *Space Astronomy Group, SSIF/ISITE Campus, ISRO Satellite Centre, Outer Ring Road, Marathahalli, Bangalore 560037, India*

18 November 2014

arXiv:1411.4135v1 [astro-ph.HE] 15 Nov 2014

**ABSTRACT**

We report the discovery of a quasi-periodic oscillation (QPO) at 642 mHz in an *XMM-Newton* observation of the ultraluminous X-ray source (ULX) IC 342 X-1. The QPO has a centroid at $\nu_{QPO} = 642 \pm 20$ mHz, a coherence factor of $Q = 11.6$, and an amplitude (rms) of 4.1% with significance of $3.6\sigma$. The energy dependence study shows that the QPO is stronger in the energy range 0.3 - 5.0 keV. A subsequent observation (6 days later) does not show any signature of the QPO in the power density spectrum. The broadband energy spectra (0.3 - 40.0 keV) obtained by quasi-simultaneous observations of *XMM-Newton* and *NuSTAR* can be well described by an absorbed *diskbb* plus *cutoffpl* model. The best fitted spectral parameters are power-law index ($\Gamma$) $\sim 1.1$, cutoff energy ($E_c$) $\sim 7.9$ keV and disc temperature ($kT_{in}$) $\sim 0.33$ keV, where the QPO is detected. The unabsorbed bolometric luminosity is $\sim 5.34\times 10^{39}$ erg s$^{-1}$. Comparing with the well known X-ray binary GRS 1915+105, our results are consistent with the mass of the compact object in IC 342 X-1 being in the range $\sim 20 - 65\ M_{\odot}$. We discuss the possible implications of our results.

**Key words:** accretion, accretion discs – black hole physics – X-rays: binaries – X-rays: individual: IC 342 X-1

## 1 INTRODUCTION

Ultraluminous X-ray sources (ULXs) are off-nuclear point X-ray sources in nearby galaxies with isotropic luminosities $> 10^{39}$ erg s$^{-1}$ (see Feng & Soria 2011 for a recent review). Since their discovery more than 30 years ago (Long & Speybroeck 1983; Fabbiano & Trinchieri 1987; Fabbiano 1988, 1989), the true nature of ULXs has remained a mystery. Early *ASCA* and *XMM-Newton* observations revealed that most ULXs should contain accreting black holes (Kubota et al. 2001; Sutton, Roberts & Middleton 2013). Recently, Motch et al. 2014 reported a firm upper limit of $< 15\ M_{\odot}$ on the mass of a black hole in a ULX suggesting that most ULXs are indeed stellar-mass black holes. However, discovery of X-ray pulsations (Bachetti et al. 2014) in one of the ULXs in M82 galaxy suggests that ULXs may also be powered by accretion onto magnetized neutron stars. In ULXs, mass estimates of the compact objects remain highly debatable because no dynamical measurement has been possible yet. However, recent optical/UV observations reveal that ULXs in M101 (Liu et al. 2013) and NGC 7793 (Motch et al. 2014) harbour stellar-mass black holes.

Since luminosities of ULXs exceed the Eddington rate for a 10 $M_{\odot}$ black hole, it has been suggested that ULXs might harbour intermediate mass black holes (IMBHs) with mass in the range $10^2 - 10^4\ M_{\odot}$ (Colbert and Mushotzky 1999; see also Pasham, Strohmayer & Mushotzky 2014). Other popular models proposed to explain the ultraluminous nature of ULXs are: (1) normal X-ray binaries (XRBs) accreting at super-Eddington rate (Begelman 2002), (2) XRBs accreting at sub-Eddington rate with beamed emission (Reynolds et al. 1997; King 2002; Begelman, King & Pringle 2006). However, the beaming scenario suffers from several difficulties, e.g, a lack of evidence of radio jets in ULXs (see Feng & Soria 2011) and the presence of a strong QPO in M82 X-1 (Strohmayer & Mushotzky 2003). Recently, Gladstone, Roberts & Done (2009) suggested a new accretion state named the *ultraluminous state* implying a super-Eddington accretion rate for ULXs. Based on the early observations with *XMM-Newton*, some ULX spectra (0.3 - 10.0 keV) were modelled with a simple

⋆ E-mail: vivekag@isac.gov.in

phenomenological model (i.e., disc emission and power-law component; Miller et al. 2003, 2004) with a characteristic disc temperature of $kT_{in} \sim 0.1$ - 0.5 keV. The presence of a cool disk component and very high luminosities, which indeed triggered the hypothesis that ULXs may contain a IMBH, may not be a valid prescription to explain most of the X-ray observational features. Recent studies (see, Gladstone, Roberts & Done 2009 for details) showed that the energy spectra can be well described by an optically thick corona ($\tau \sim 5 - 30$, whereas $\tau \sim 1$ for corona seen in Galactic black hole binaries) coupled with an accretion disc. In addition, the presence of a high-energy curvature (> 3.0 keV), not seen in Galactic black hole binaries (Remillard & McClintock 2006) accreting at a sub-Eddington rate, is now considered as one of the ULX spectral signatures (Stobbart, Roberts & Wilms 2006; Gladstone, Roberts & Done 2009). Furthermore, combining both spectral and temporal variabilities, Sutton, Roberts & Middleton (2013) classified three spectral regimes for ULXs, namely *broadened disc*, *hard ultraluminous* and *soft ultraluminous* class. Recently, Pintore et al. (2014) investigated a larger sample of observations for studying the spectral evolution with a different approach (i.e., based on *colour-colour* and *hardness-intensity diagram* analysis). All these studies further corroborate the idea of a new accretion state (i.e., *ultraluminous state*) for ULXs (Roberts 2007; Gladstone, Roberts & Done 2009).

The study of short-term variability may also put constraints on the various accretion models in ULXs (see Pasham, Strohmayer & Mushotzky 2014). In a few ULXs (M82 X-1, NGC 5408 X-1, NGC 6946 X-1, M82 X42.3+59), QPOs have been detected in the frequency range of $\sim$ 3 mHz to 200 mHz (Strohmayer & Mushotzky 2003; Dewangan et al. 2006a; Strohmayer et al. 2007; Rao, Feng & Kaaret 2010; Feng, Rao & Kaaret 2010; Pasham & Strohmayer 2012). A QPO around 200 mHz has been reported in Holmberg X-1 (Dewangan, Griffiths & Rao 2006b), but was not confirmed later (see Heil, Vaughan & Roberts 2009). Recently, Pasham, Strohmayer & Mushotzky (2014) reported twin-peak QPOs in M82 X-1 at frequencies of 3.32 and 5.07 Hz. Several ULXs show the short-term variability with (or without) the presence of QPOs in the power spectra, whereas the variability is found to be completely suppressed in some sources (Heil, Vaughan & Roberts 2009). It has been suggested that the short-term variability in the ultraluminous state can be produced by variable obscuration due to clumpy winds (see Middleton et al. 2011; Sutton, Roberts & Middleton 2013).

IC 342 X-1 is a ULX in the nearby spiral galaxy IC 342 at a distance of 3.3 Mpc (Saha et al. 2002). The source was discovered by the *Einstein* satellite (Fabbiano & Trinchieri 1987). This source was also detected by *ROSAT* in the ultra-luminous state (Bregman, Cox & Tomisaka 1993; Roberts & Warwick 2000). *ASCA* observations of the source taken during 1993 and 2000 revealed spectral transitions from a high/soft to a low/hard spectrum (Kubota et al. 2001). The analysis carried out using *Suzaku*, *XMM-Newton*, *Chandra* and *Swift* revealed two different power-law (PL) states in this source (Yoshida et al. 2013): low-luminosity PL state and high luminosity PL state. Recently, Marlowe et al. (2014) reported a clear change in a recent

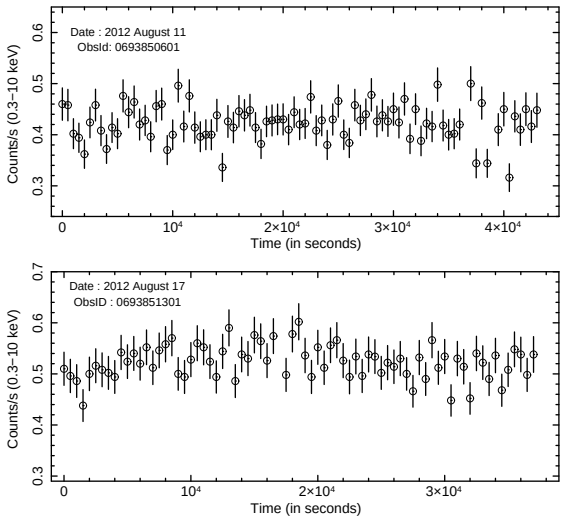


**Figure 1.** Photon counts variation of IC 342 X-1 observed with *XMM-Newton* (EPIC-pn data) in the energy band of 0.3 - 10.0 keV. **Top panel**: The start time of observation was (Obs-1) 2012-08-11 20h 30m 47s (UT); **Bottom panel**: The start time of observation was (Obs-2) 2012-08-17 20h 12m 45s (UT). Each data point corresponds to 500 sec time bin.

*Chandra* spectrum with a much softer spectrum than seen in all previous observations and it has been modelled with a standard accretion disc emission. The source has also been detected in radio using VLA, but the presence of a compact radio jet was not confirmed in the high spatial resolution data as observed with VLBI (Cseh et al. 2012).

In the present work, we focus on the recent quasi-simultaneous observations of IC 342 X-1 made by *XMM-Newton* and *NuSTAR* in August 2012. Recently, Rana et al. (2014) also analysed the same data sets in order to understand the broadband spectral nature of the source. From our detailed analysis (see §2 & §3), we report the detection of QPO in IC 342 X-1 along with the spectral properties of the source.

## 2 OBSERVATION AND DATA REDUCTION

*XMM-Newton* observed IC 342 X-1 six (6) times between 2001 and 2012. We use the data obtained on 2012 August 11 with an exposure time of 55 ks (Obs-1) and on 2012 August 17 for a total exposure of 50 ks (Obs-2). The previous data sets (i.e., initial four observations) have been analyzed by Yoshida et al. (2013) (see Pintore et al. 2014 for recent analysis). The 2012 observations were carried out in *PrimeFullWindow* mode with a time resolution of 73.35 ms. Data reduction is performed using Science Analysis System (SAS) Version 12.0.1 and using the recent calibration data set. We create the calibrated event files using SAS task *epchain*. We extract the lightcurve from the entire chip in the 10.0 - 15.0 keV band and then generate the gti file using the selection criteria (rate <= 3 × the mean of the 10.0 - 15.0 keV lightcurve). We select EPIC-pn events with $PATTERN <= 4$ and $FLAG == 0$. We use a circular region of 40″ centered at the source position to extract the source events. A circular region of similar size away from the source position is used to extract the background events. We

apply the gti filter while creating the lightcurves in the 0.3 - 10.0 keV, 0.3 - 5.0 keV and 5.0 - 10.0 keV bands for Obs-1 and Obs-2. We find that the above filtering process removes the large background flares at the end of the observations. We also observe that the filtering process produces two data gaps of 500 s and 300 s in the lightcurves of Obs-1 corresponding to two short flares and **a** 300 s data gap in the lightcurves of Obs-2.

The task *rmfgen* and *arfgen* are used to create response matrix file (rmf) and ancillary response file (arf). The spectra are grouped to give a minimum of 25 counts/bin.

*NuSTAR* also observed the source on 2012 August 10 for a total exposure time of 98.6 ks and 2012 August 16 for a total exposure of 127.3 ks. We use the most recent *NuSTAR* analysis software distributed with HEASOFT version 6.15 and the latest calibration file**s** (version 20131007) for reduction and analysis of the *NuSTAR* data. We use **the** task *nupipeline* to generate calibrated and screened event files. A circular region of 30″ centered at the source position is used to extract the source events. Background events are extracted from a circular region of same size away from the source. The task *nuproduct* is used to generate the spectra and response files. The spectra are grouped to give a minimum of 25 counts/bin.

## 3 ANALYSIS AND RESULTS

The background subtracted lightcurves of IC 342 X-1 observed with *XMM-Newton* at two different epochs (Obs-1 & Obs-2) are shown in Figure 1 with effective exposure times (resulted after removing the high background intervals) of 43.5 ksec and 37.5 ksec respectively. The average count rate for Obs-1 is $0.40 \pm 0.02$ and that for Obs-2 is $0.51 \pm 0.02$. The variability of about 20% is evident in both observations on time scale of few 1000 seconds. The average count rates between two observations also vary by $\sim 30\%$.

### 3.1 Power Density Spectrum

We compute the power density spectra (PDS) from the background subtracted lightcurves using the EPIC-pn data. We follow the procedure given in Heil, Vaughan & Roberts (2009) to construct the PDS. We fill the telemetry gaps (> 15 s) and gaps due to the short flares with local averages. We use a binsize of 0.220 s (3 times the temporal resolution) to construct the PDS. We divide the entire lightcurve into intervals of 256 bins (56.32 s) and compute the PDS for each interval independently. Then we co-add all the PDS and average them in a single frame. The final PDS is rebinned geometrically in frequency space by a factor of 1.04.

Figure 2a and Figure 2d show the Leahy power spectra (0.3 - 10.0 keV) for both observations (Obs-1 & Obs-2). The PDS of Obs-1 (Fig. 2a) show**s** a QPO at centroid frequency $\sim 642$ mHz. The PDS of Obs-2 (Fig. 2d) does not show any signature of QPO like feature. The PDS in the 0.3 - 5.0 keV range shows QPO at 653 mHz (Fig. 2b). However, no QPO is observed in the 5.0 - 10.0 keV power spectrum (Fig. 2c).

We fit the PDS in the 0.3 - 10.0 keV and 0.3 - 5.0 keV bands (for Obs-1) with a model composed of a Lorentzian for a QPO peak, a power-law ($AE^{-\alpha}$, $\alpha = 1.5 \pm 0.8$ for the 0.3 - 10.0 keV band, $\alpha = 1.95 \pm 0.9$ for the 0.3 - 5.0 keV

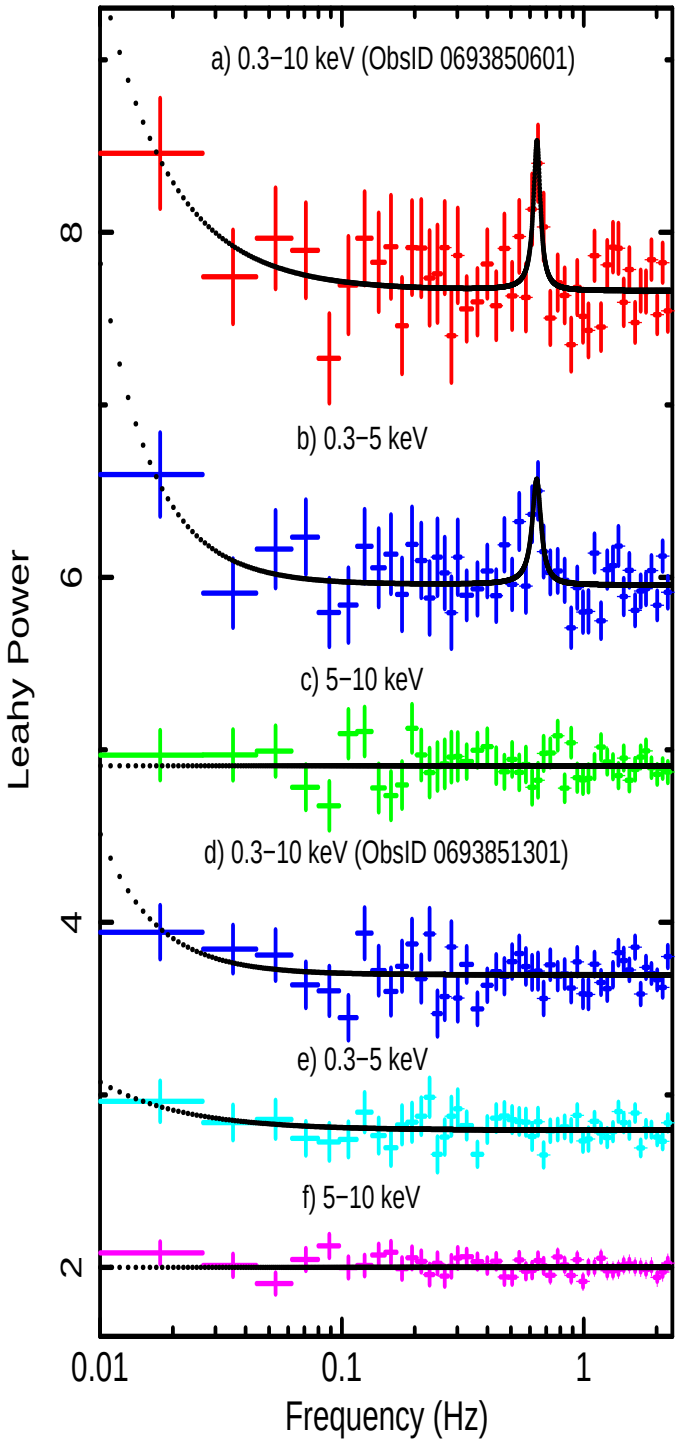


**Figure 2. a)** The Leahy normalized power density spectrum for Obs-1 in the 0.3 - 10.0 keV band computed using EPIC-pn data. The PDS has been fitted with a Lorentzian for QPO feature, a power-law and a constant to account for the Poissonian noise. The Poissonian noise has not been subtracted. **b)** The Leahy normalized power density spectrum for Obs-1 in the 0.3 - 5.0 keV band. A clear QPO feature fitted with Lorentzian is seen. **c)** The Leahy normalized power density spectrum for Obs-1 in the 5.0 - 10.0 keV band. **d)** The Leahy normalized power density spectrum for Obs-2 in the 0.3 - 10.0 keV band without any signature of QPO like feature. **e)** The Leahy normalized power density spectrum for Obs-2 in the 0.3 - 5.0 keV band. **f)** The power spectrum for Obs-2 in the 5.0 - 10.0 keV band. See text for details.

band) and a constant to account for the Poissonian noise. We get $\chi^2_{red} = 1.02$ ($\chi^2/dof = 45/44$) for the 0.3 - 10.0 keV band and $\chi^2_{red} = 1.06$ ($\chi^2/dof = 47/44$) for the 0.3 - 5.0 keV band. The resultant fits are shown in Fig. 2a and Fig. 2b respectively. Fitting the power spectra (Obs-1) in the 0.3 - 10 keV and 0.3 - 5.0 keV bands with a power-law and a constant gives $\chi^2_{red} = 1.51$ ($\chi^2/dof = 71/47$) and $\chi^2_{red} = 1.57$ ($\chi^2/dof = 74/47$) respectively. So, overall fitting is improved upon considering the Lorentzian component for the QPO feature. Fitting the power spectra of Obs-2 in the 0.3 - 10.0 keV and 0.3 - 5.0 keV bands with a power-law and a constant gives $\chi^2_{red} = 1.22$ ($\chi^2/dof = 57/47$) and $\chi^2_{red} = 1.02$ ($\chi^2/dof = 48/47$) respectively. We note that no Lorentzian component is required to improve the fit of the PDS of Obs-2 in both energy bands (see Fig. 2d, 2e). We also note that the PDS in the 5.0 - 10.0 keV energy bands for both observations (Obs-1 and Obs-2) are featureless and can be fitted with a constant to account for the Poissonian noise (see Fig. 2c, 2f). The significance of the QPO parameters in both bands are estimated with F-test statistics. The best fit model in the 0.3 - 10.0 keV band gives a QPO of centroid frequency $\nu_{QPO} = 642 \pm 20$ mHz, a Q-factor ($\nu/FWHM$) = 11.6 and an amplitude (rms) of 4.1% with significance of $3.6\sigma$. The best fit QPO parameters in the 0.3 - 5.0 keV band are centroid frequency $\nu_{QPO} = 653 \pm 30$ mHz, Q-factor = 9.8 and amplitude (rms) of 4.5%. The QPO in the 0.3 - 5.0 keV band is detected with a significance of $3.7\sigma$. The total integrated power (0.01 - 2.5 Hz) is $\sim$ 7.2% in the energy band of 0.3 - 10.0 keV for Obs-1 and 3.2% for Obs-2. All errors quoted are computed using $\Delta\chi^2 = 1.0$.

Note that considering the time interval (Obs-1) before the short flares results in 36.5 ks continuous observation. The PDS created using this exposure time (36.5 ks) shows a QPO feature with similar parameters. However, the significance of the QPO changes from 3.6 to $3.4\sigma$.

### 3.2 Energy Spectrum

The energy spectra of EPIC-pn and *NuSTAR/FPMA* are analysed using XSPEC version 12.8.1. We fit the combined EPIC-pn (0.3 - 10.0 keV band; Obs-1) and *NuSTAR*/FPMA (3.0 - 40.0 keV; 2012 August 10) data (epoch-1) with: 1) *power-law*, 2) power-law with exponential cut-off (*cutoffpl* in XSPEC), 3) *cutoffpl* with an addition of multi-temperature disk component for the standard thin accretion disk (*diskbb* in XSPEC; Mitsuda et al. 1984), 4) *diskbb* plus Comptonization model (*compTT* model of XSPEC; Titarchuk 1994). We consider the *tbabs* model (Wilms, Allen & McCray 2000) for all the spectral models in order to model the extinction ($N_H$) on the line of sight to the source. Similarly, the second quasi-simultaneous data (epoch-2) obtained with EPIC-pn (0.3 - 10.0 keV; Obs-2) and *NuSTAR*/FPMA (3.0 - 40.0 keV; 2012 August 16) are also analyzed and fitted with above mentioned models. The cross-calibration constant between *NuSTAR/FPMA* and *XMM-Newton/EPIC-pn* is found to be close to 1 ($\sim$ 0.95).

The best fit parameters for all the models are listed in Table 1. All errors quoted are computed using $\Delta\chi^2 = 1.0$ (at 68% confidence). The $N_H$ values are found to be in the range of 0.5 - 0.7 $\times 10^{22}$ $cm^{-2}$(see Table 1). For epoch-1, the *power-law* and *cutoffpl* model give $\chi^2_{red} = 1.22$ ($\chi^2/dof =$ 785/643) and $\chi^2_{red} = 1.10$ ($\chi^2/dof = 706/642$) respectively. The probability that the fit is improved by chance is 1.59 $\times$ $10^{-16}$. Hence a simple *power-law* model is not the best description of the data and the spectrum shows a clear high energy cutoff. Since **a** soft excess modelled with the *diskbb* has been observed in many ULXs (Miller et al. 2003, 2004; Feng & Kaaret 2005; Stobbart, Roberts & Wilms 2006), we fitted the epoch-1 spectrum with the *diskbb+cutoffpl* model. The fit results in $\chi^2_{red} = 0.99$ ($\chi^2/dof = 634/640$) and chance improvement probability equals to 1.12$\times$ $10^{-15}$ for inclusion of the *diskbb* component, suggesting that a soft excess component below 2 keV is required to improve the fit.

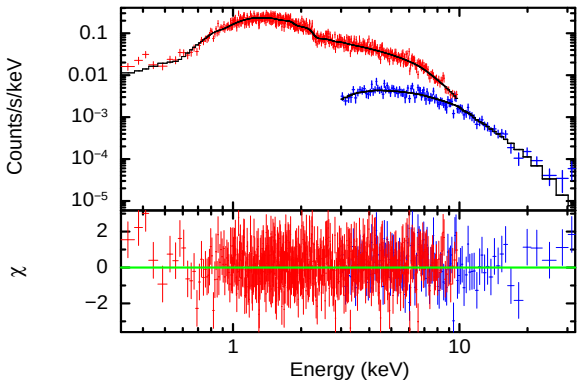


**Figure 3.** The combined EPIC-pn (for Obs-1) and *NuSTAR/FPMA* (on August 10 2012) spectrum and folded model (top panel). The spectrum has been modeled with an absorbed *diskbb* plus *cutoffpl* model. The residuals in unit of sigma is shown in the bottom panel.

Analysis of XMM-Newton data of several ULXs revealed that the disc emission plus cool ($kTe \sim 3$ keV) and optically thick ($\tau \sim 5$ - 30) Comptonized component models the spectral data well (Gladstone, Roberts & Done 2009). Hence, we tried with the *compTT* model also instead of *cutoffpl*. The combination of *diskbb* plus *compTT* model, where the seed photon temperature is tied to the inner disc temperature, gives $\chi^2_{red} = 1.01$ ($\chi^2/dof = 645/640$). Hence, the *diskbb+cutoffpl* model is the best description for the epoch-1 observation. epoch-2 data can also be well modelled with the *diskbb+cutoffpl* model resulting in $\chi^2_{red} = 1.04$ ($\chi^2/dof$ = 729/699).

The disc temperature is 0.33 $\pm$ 0.03 keV and 0.47 $\pm$ 0.06 keV respectively for the epoch-1 and epoch-2 data. The *diskbb* normalization is found to be unphysically small for both spectra. The cutoff energy ($E_c$) is 7.92 $\pm$ 0.91 keV and 7.27 $\pm$ 0.99 keV respectively for epoch-1 and epoch-2 spectra (see also Rana et al. 2014). Although the *diskbb+cutoffpl* model is the best description of the spectra, the *diskbb+compTT* model also provides statistically good description of the spectra for both epochs. The best fit optical depth ($\tau$) and electron temperature ($kT_e$) for the epoch-1 spectrum are 13.32 $\pm$ 0.66 and 3.35 $\pm$ 0.17 keV respectively. The best fit $\tau$ and $kT_e$ for the epoch-2 are 12.31 $\pm$ 0.41 and 3.29 $\pm$ 0.15 keV respectively.

In Table 1, we also give the estimated unabsorbed total flux in 0.1 - 100.0 keV band and corresponding luminosities for all the models using a distance of 3.3 Mpc. The unab-

sorbed fluxes and corresponding errors are computed using the convolution model *cflux* of XSPEC.

## 4 DISCUSSION AND SUMMARY

In the present work, we report the discovery of a QPO in the *XMM-Newton* data of the ULX source IC 342 X-1, a system harbouring a black hole (see Okada et al. 1998). The detection of a peak at $\sim 642$ mHz (Q $\sim 11.6$, rms $\sim 4.1\%$ and significance $3.6\sigma$) in the power spectrum of IC 342 X-1 (Obs-1) could be used to constrain the mass of the 'hole' as this technique was employed for other ULXs (Dewangan et al. 2006a; Strohmayer et al. 2007; Rao, Feng & Kaaret 2010). Interestingly, the QPO detection in IC 342 X-1 is also the highest frequency observed in a ULX to date, whereas the subsequent *XMM-Newton* observation (6 days later) does not show any signature of QPO like feature.

Detailed spectral analysis shows that the broadband spectrum (0.3 - 40.0 keV) of the source (epoch-1) is well described by an absorbed *diskbb* plus a *cutoffpl* or with a *diskbb* plus a *compTT* model. The best fit model parameters indicate that the source was in a hard spectral state ($\Gamma \sim 1.04$, $\tau \sim 13.32$, $E_c \sim 7.92$ keV) that is unlike the canonical hard state as commonly seen in Galactic black hole binaries (GBHBs). The unabsorbed luminosity of the source is found to be around $\sim 5.34 \times 10^{39}$ erg s$^{-1}$. Similar spectral features are also seen in the epoch-2 observation. All these observational results are consistent with the findings of Gladstone, Roberts & Done (2009) and implies that the source could be in the hard ultraluminous state (Sutton, Roberts & Middleton 2013).

In general, the power spectra of GBH sources are characterized by various broad noise components (power-law like red noise, flat-top noise etc.) along-with a narrow noise component (i.e. Lorentzian type for QPO like feature). The high temporal variability and low frequency QPOs ($\sim 0.1 - 20$ Hz) observed in BH sources are mostly associated with the hard or intermediate states. In general, the low frequency QPOs seen in Galactic BHs are classified as A, B and C type (Casella et al. 2005). As an example, the C-type QPO has a high Q-factor (6 - 12), a large amplitude (3% - 16% rms) and shows complex phase lag behaviour along with flat-top noise component. Moreover, the low frequency QPOs evolve with the spectral states and completely disappear in the thermally dominated soft state (Remillard & McClintock 2006; Nandi et al. 2012). Since the QPOs scale inversely with the mass of a black hole in GBH sources (Shrader and Titarchuk 2003; Shaposhnikov & Titarchuk 2009), the observed QPOs can be used to infer the mass of the putative black hole.

In contrast, the nature of the power spectra and short-term variability are more complex in ULXs (Heil, Vaughan & Roberts 2009). Few sources show signatures of QPOs without any change in the centroid QPO frequency (except M82 X-1, see Feng & Soria 2011 for details). The recent discovery of twin-peak X-ray QPOs (3:2 frequency ratio) in M82 X-1 is found to be stable (see Pasham, Strohmayer & Mushotzky 2014). No definite correlation exists between the QPOs and spectral states in ULXs, but a defined correlation exists for most GBHBs. In the case of IC 342 X-1, the power spectrum of Obs-1 can be modelled with a constant and a Lorentzian feature (for QPO) along with a power-law component. The observed intrinsic variability is around $\sim 7.2\%$. This form of PDS is a common characteristic of ULXs (see Heil, Vaughan & Roberts 2009), where significant variability is observed and the power spectra are modelled with a power-law or with a broken power-law component. Interestingly, the power spectrum of Obs-2 (6 days later) does not show any presence of a QPO but both observations (Obs-1 & Obs-2) show similar spectral nature (see Table 1).

Another important thing to note **is** that the hard X-ray energy spectra of GBHBs (i.e., hard or intermediates states) have connection with the strong QPOs and compact radio jets observed in the sources (Radhika & Nandi 2014). The high energy spectral curvatures observed in GBHBs (in the range of 30 - 100 keV) are the manifestation of optically thin corona with characteristic temperature of $\sim 100$ keV (Remillard & McClintock 2006). However, in ULXs the spectral nature is quite different with spectral curvature of electron temperature of few keV and optical depth in the range of 5 to 30 (thick corona). Also, the connection between the hard X-ray spectral nature, the QPOs and compact jets is not well established in ULXs. So, it is hard to compare the spectral nature of ULXs with that of GBHBs.

Since the characteristic time-scale of active galactic nuclei (AGNs) or a GBH scales with the compact object mass (McHardy et al. 2006), one can raise the following basic question - could the observed QPO in IC 342 X-1 be analogous to any type of QPOs observed in Galactic black holes? There have been several attempts to identify the QPOs seen in ULXs (Strohmayer & Mushotzky 2009; Pasham & Strohmayer 2012; Feng, Rao & Kaaret 2010) with those seen in GBHBs. However, the classification of QPOs observed in ULXs remains unclear (Middleton et al. 2011). The detection of 642 mHz QPO in IC 342 X-1 which shows some of the characteristics (Q-factor = 11.6 and rms = 4.1%) of C-type QPO, can be used to constrain the black hole mass in IC 342 X-1. However, true classification requires phase lag study which is beyond the scope of the present work. The heaviest Galactic BH source GRS 1915+105 (Greiner, Cuby & McCaughrean 2001) shows C-type QPOs in the frequency range 1 - 3 Hz. If we consider that the 642 mHz QPO is a scaled-down version of the QPOs seen in GRS 1915+10 along with the assumption that the QPO frequencies scale inversely proportional to the BH masses (Remillard & McClintock 2006), then we can estimate the black hole mass in IC 342 X-1 as $M_{BH}(IC342X-1) \sim \nu_{QPO}(GRS1915)/\nu_{QPO}(IC342X-1) \times M_{BH}(GRS1915) \sim 20 - 65\ M_{\odot}$ (considering the mass of GRS 1915+105 $\sim 14\ M_{\odot}$). It implies that for the bolometric luminosity $\sim 5.34 \times 10^{39}$ erg s$^{-1}$, the black hole at the centre of IC 342 X-1 is accreting matter at near-Eddington rate ($\sim 0.7 - 2\ L_{Edd}$).

Another possibility for estimating the mass of the black hole in IC 342 X-1 is to consider the observed QPO as a scaled-down version of those HFQPOs which are observed in GBHBs (eg. 65-67 Hz in GRS 1915+105; see Morgan, Remillard and Greiner 1997; 66 Hz in IGR J17091-3624; see Altamirano & Belloni 2012). In this scenario, the estimated mass could be in the range of $\sim 1000 - 1800\ M_{\odot}$ (considering the mass of GRS 1915+105 $\sim 14 \pm 4\ M_{\odot}$). It would imply that the central black hole accretes matter at sub-Eddington rate (0.02 - 0.05 $L_{Edd}$). This may not be

**Table 1.** Summary of the spectral fits ($\Gamma$ is photon index, $E_c$ is cutoff energy, $kT_{in}$ is disk temperature, $N_{dbb}$ is disk normalization, $kT_e$ is electron temperature of corona, $\tau$ is optical depth of corona. $F_{tot}$ is total flux in units of $10^{-12}$ erg/s/cm$^2$, $L_{tot}$ is total luminosity in units of $10^{39}$ erg/s). Errors quoted are calculated at 68% confidence level.

| | epoch-1 | | | | epoch-2 | | | |
|---|---|---|---|---|---|---|---|---|
| Parameters | power-law | cutoffpl | diskbb+cutoffpl | diskbb+compTT | power-law | cutoffpl | diskbb+cutoffpl | diskbb+compTT |
| $N_H$ ($\times$ $10^{22}$ cm$^{-2}$) | 0.61±0.01 | 0.54±0.01 | 0.64±0.03 | 0.67±0.06 | 0.71±0.03 | 0.61±0.02 | 0.59±0.02 | 0.51±0.04 |
| $\Gamma$ | 1.82±0.02 | 1.51±0.04 | 1.04±0.10 | – | 2.04±0.02 | 1.66±0.04 | 1.12±0.18 | – |
| $E_c$ (in keV) | – | 15.93±1.7 | 7.92±0.9 | – | – | 13.45±1.2 | 7.27±0.95 | – |
| $kT_{in}$ (in keV) | – | – | 0.33±0.03 | 0.23±0.03 | – | – | 0.47±0.06 | 0.29±0.02 |
| $N_{dbb}$ | – | – | $4.96^{+3.8}_{-1.1}$ | $28^{+30.8}_{-10.4}$ | – | – | 1.08±0.3 | $3.12^{+3.01}_{-1.21}$ |
| $kT_e$ (in keV) | – | – | – | 3.35±0.17 | – | – | – | 3.29±0.15 |
| $\tau$ | – | – | – | 13.32±0.66 | – | – | – | 12.31±0.41 |
| $F_{tot}$ (0.1-100 keV) | 8.91±0.08 | 5.05±0.06 | 4.21±0.11 | 4.46±0.05 | 8.49±0.12 | 5.88±0.09 | 4.21±0.2 | 4.36±0.3 |
| $L_{tot}$ (0.1-100 keV) | 11.56±0.01 | 6.55±0.07 | 5.34±0.14 | 5.78±0.06 | 11.01±0.02 | 7.62±0.01 | 5.31±0.25 | 5.65±0.26 |
| $\chi^2$/dof | 785/643 | 706/642 | 634/640 | 645/640 | 884/702 | 756/701 | 729/699 | 736/699 |

the case for IC 342 X-1, as the observed spectral properties favour the *hard ultraluminous state* of ULXs, explained by a system harbouring a stellar-mass black hole accreting at and above the Eddington limit (Gladstone, Roberts & Done 2009; Sutton, Roberts & Middleton 2013).

We are then left with the possibility that the central 'hole' of IC 342 X-1 might be harbouring a 'massive' stellar-mass black hole of mass $\sim 20-65\ M_\odot$. The present stellar evolution models also predict massive BH remnants ($\sim 20-100\ M_\odot$) that could be formed from direct collapse of the progenitor without any supernova explosion (Fryer 1999).

## ACKNOWLEDGMENTS

Authors would like to thank the anonymous referee for his/her careful reading of the paper, and constructive criticism along with useful suggestions for improvement of the manuscript. We also would like to thank Dr. Girish and Dr. Das for careful reading and comments on the manuscript. This research has made use of data and/or software provided by the High Energy Astrophysics Science Archive Research Center (HEASARC). We thank Dr. Anil Agarwal, GD, SAG, Mr. Vasantha E. DD, CDA and Dr. S. K. Shivakumar, Director, ISAC for encouragement and continuous support to carry out this research.

## REFERENCES

Altamirano D., Belloni T., 2012, ApJ, 747,L4
Bachetti M., Harrison F. A., Walton D. J, et al., 2014, Nature, 514, 202
Begelman M. C., 2002, ApJ, 568, L97
Begelman M. C., King A. R., Pringle J. E. 2006, MNRAS, 370, 399
Belloni T. M., Altamirano D., 2013, MNRAS, 432, 10
Bregman J. N., Cox C. V., Tomisaka K., 1993, ApJ, 415, L79
Casella P., Belloni T., Stella L., 2005, ApJ, 629, 403
Colbert E. J. M., Mushotzky R. F., 1999, ApJ, 519, 89
Cseh D., Corbel S., Kaaret P., Lang C., Grise F., Paragi Z., Tzioumis A., Tudose V., et al., 2012 ApJ, 749, 17
Dewangan G. C., Titarchuk L., Griffiths R. E., 2006a, ApJ, 637, L21
Dewangan G. C., Griffiths R. E., Rao A. R., 2006b, ApJ, 641, L125.
Fabbiano G., Trinchieri G. 1987, ApJ, 315, 46
Fabbiano G., 1988, ApJ, 325, 544
Fabbiano G., 1989, ARA&A, 27, 87
Feng H., Rao F., Kaaret P., 2010, ApJ, 710, L137
Feng H., Soria R., 2011, New Astronomy Rev., 55, 166
Feng H., Kaaret P., 2005, ApJ, 633, 1052
Fryer C. L., 1999, ApJ, 522, 413
Greiner J., Cuby J. G., McCaughrean M. J., 2001, Nature, 414, 522
Gladstone J. C., Roberts T. P., Done C., 2009, MNRAS, 397, 1836
Heil L. M., Vaughan S., Roberts T. P., 2009, MNRAS, 397, 1061
King A. R., 2002, MNRAS, 335, L13
Kubota A., Mizuno T., Makishima K., Fukazawa Y., Kotoku J., Ohnishi T., Tashiro M., 2001, ApJ, 547, L119
Liu J., Bregman J. N., Bai Y., Justham S., Crowther P., 2013, Nature, 503, 500
Long K. S., van Speybroeck L. P. 1983, in Accretion-Driven Stellar X-ray Sources, ed. W. H. G. Lewin & E. P. J. van den Heuvel, 117-146
Marlowe H., Kaaret P., Lang C., Feng H., et al., 2014, MNRAS, 444, 642
McHardy I. M., Koerding E., Knigge C., Fender R. P., 2006, Nature, 444, 730
Middleton M. J., Roberts T. P., Done C., Jackson F. E., 2011, MNRAS, 411, 644
Miller J. M., Fabbiano G., Miller M. C., Fabian A. C., 2003, ApJ, 585, L37
Miller J. M., Fabian A. C., Miller M. C., 2004, ApJ, 607, 931
Mitsuda K., Inoue H., Koyama K., et al., 1984, PASJ, 36, 741
Morgan E. H., Remillard R. R., Greiner J., 1997, ApJ,482, 993
Motch C., Pakull M., Soria R., Grise F., Pietrzynski G., 2014, Nature, 514, 198
Nandi A., Debnath D., Mandal S., Chakrabarti S. K., 2012, A&A, 542, 56
Okada K., Dotani T., Makishima K., et al. 1998, PASJ, 50, 25
Rao F., Feng H., Kaaret P., 2010, ApJ, 722, 620
Pasham D. R., Strohmayer T. E., 2012, ApJ, 753, 139

Pasham D. R., Strohmayer T. E., Mushotzky R. F., 2014, Nature, 513, 74
Pintore F., Zampieri L., Wolter A., Belloni T., 2014, MNRAS, 439, 3461
Radhika D., Nandi A., 2014, AdSpR, 54, 1678
Rana V., Harrison F. A., Bachetti M., Walton D.J., Furst F., Barret D. Miller J.M., 2014, astroph/1401.4637
Remillard R. A., McClintock J. E., 2006, ARA&A, 44, 49
Reynolds C. S., Loan A. J., Fabian A. C., Makishima K., Brandt W. N., Mizuno T., 1997, MNRAS, 286, 349
Roberts T. P., 2007, Ap&SS, 311, 203
Roberts T. P., & Warwick R. S., 2000, MNRAS, 315, 98
Saha A., Claver J., Hoessel, J. G., 2002, AJ, 124, 839
Shaposhnikov N., Titarchuk L., 2009, ApJ, 699, 453
Shrader C. R., Titarchuk L., 2003, ApJ, 598, 168
Stobbart A.-M., Roberts T. P., Wilms, J., 2006, MNRAS, 368, 397
Strohmayer T. E., Mushotzky R. F., 2003, ApJ, 586, L61
Strohmayer T. E., Mushotzky R. F., Winter L., Soria R., Uttley P., Cropper, M., 2007, ApJ, 660, 580
Titarchuk L., 1994, ApJ, 434, 570
Strohmayer T. E., Mushotzky R. F., 2009, ApJ, 703, 1386
Sutton A. D., Roberts T. P., Middleton M. J., 2013, MNRAS, 435, 1758
Yoshida T., Isobe N., Mineshige S., Kubota A., Mizuno T., Saitou K., 2013, PASJ, 65, 48
Wilms J., Allen A., McCray R., 2000, ApJ, 542, 914